ELSEVIER

Journal of Nuclear Materials 283–287 (2000) 306–312

journal of nuclear materials

www.elsevier.nl/locate/jnucmat

Microstructure of Cu–Ni alloys neutron irradiated at 210°C and 420°C to 14 dpa

S.J. Zinkle [a,*], B.N. Singh [b]

[a] Metals and Ceramics Division, Oak Ridge National Laboratory, P.O. Box 2008, Oak Ridge, TN 37831-6138, USA

[b] Materials Research Department, Risø National Laboratory, DK 4000 Roskilde, Denmark

Abstract

Transmission electron microscope (TEM) disks of pure copper and copper containing 0.17–10% Ni were neutron irradiated at 210°C and 420°C in Hf-shielded capsules in the High Flux Isotopes Reactor to doses of 13.5 and 14.9 displacements per atom (dpa), respectively. Void swelling was not observed in any of the specimens irradiated at 210°C. Instead, a high density of stacking fault tetrahedra (SFTs) and a moderate density of dislocation loops were observed. There was no evidence for defect cluster patterning (wall formation) in any of the specimens irradiated at 210°C. The SFT density was independent of Ni content, whereas the loop density was highest in the alloy containing ~2% Ni. Pronounced void swelling was observed in all of the specimens irradiated at 420°C. A void denuded zone of ~2 μm width was observed adjacent to grain boundaries. The void swelling in copper containing ~2% Ni showed a pronounced maximum in a 10-μm wide band adjacent to the grain boundary denuded zones. Matrix voids aligned along ⟨1 1 0⟩ directions were observed in Cu–10%Ni irradiated at 420°C. The occurrence of the peak swelling zone and the partial ordering of voids are both consistent with the predictions of the recent production bias model which includes 1-D diffusional transport of clusters of self-interstitial atoms.

1. Introduction

Previous neutron [1–6], ion [7–9] and electron [10] irradiation studies have found that void swelling is reduced in Cu–Ni alloys compared to pure copper, particularly for electron and ion irradiations. Suppressed swelling has also been observed for neutron irradiation temperatures below 400°C and Ni additions >2%. In particular, the void swelling in Cu and Cu–Ni alloys irradiated to 11 displacements per atom (dpa) at 373°C decreases rapidly with increasing Ni content (~8% swelling for pure Cu vs. 1% to −1% swelling for copper containing 2–10% Ni) [11]. On the other hand, the high-dose swelling of neutron-irradiated Cu and Cu–Ni alloys appears to be comparable at irradiation temperatures above 400°C [4,12]. The addition of Ni solute has been found to produce a reduction in void density compared to pure copper [1–3]. Conflicting results have been obtained between electron and neutron irradiations regarding void size. The void size under neutron irradiation conditions is higher in the Cu–Ni alloys, whereas the largest voids under electron irradiation were observed in pure copper. According to the ion irradiation results by Muroga et al. [9], the addition of Ni causes an upward shift in the peak swelling temperature of copper alloys. Nickel segregation to void surfaces and grain boundaries has been observed in electron- [13,14] and neutron- [3,5,6] irradiated Cu–Ni alloys.

The objective of this study was to examine the effect of Ni additions on defect cluster (SFT, dislocation loop, void) formation in neutron-irradiated copper. Although the irradiation behavior of copper and copper alloys has been extensively studied up to high doses (>100 dpa) for irradiation temperatures of ~400–500°C, very little is known about the high-dose radiation response of copper and Cu alloys at fusion-relevant temperatures of 50–300°C [6,15].

* Corresponding author. Tel.: +1-865 576 7220; fax: +1-865 241 3650.

E-mail address: zinklesj@ornl.gov (S.J. Zinkle).

PII: S0022-3115(00)00359-7

2. Experimental procedure

All of the specimens were prepared as TEM disks with dimensions 3 mm diameter by 0.1 mm thickness. The OFHC Cu disks (99.999% purity, Tréfimétaux) were vacuum annealed at 550°C for 2 h after fabrication (20 μm grain size). The Cu–Ni alloys containing 0.17%, 1%, 2%, 5% and 10% Ni (Harwell, UKAEA) were vacuum annealed at 800°C for 4 h. The grain sizes for the Cu–Ni alloys decreased with increasing Ni content, with measured values of 150, 105, 90 and 27 μm for alloys containing 1%, 2%, 5% and 10% Ni.

The specimens were irradiated in TEM disk packets in the High Flux Isotopes Reactor at ORNL as part of the HFIR-MFE-200J-1 and -400J-1 irradiation capsules, which operated at average irradiation temperatures of 200°C and 400°C, respectively [16]. Based on continuous in-core thermocouple measurements, the temperatures of the Cu alloy TEM specimens varied during the irradiation from 205°C to 215°C and 415°C to 425°C for the two capsules. The specimens were irradiated for 440.6 effective full-power days to fast neutron fluences of 1.76 and 1.94×10^{26} n m^{-2} ($E > 0.1$ MeV) [17], which corresponds to damage levels of 13.5 and 14.9 dpa in copper for the 210°C and 420°C specimens, respectively. The damage rate was 3.5×10^{-7}–3.9×10^{-7} dpa s^{-1} for the two irradiation temperatures. The capsules were surrounded by hafnium shielding (4.2 mm thick), which reduced the midplane thermal neutron flux to 9.2×10^{18} n m^{-2} s^{-1}, i.e., ~20% of the unshielded value. Further irradiation details are given elsewhere [16,17]. The calculated dominant solute transmutations in copper for the 14 dpa irradiations are 1.4% Ni and 0.5% Zn. The irradiation produced transmutation He levels ranging from 2 appm in Cu to 22 appm in Cu–10%Ni [17]. The helium production in the Ni-bearing alloys was mainly from the ^{58}Ni(n,γ)^{59}Ni(n,α)^{56}Fe two-step reaction.

The irradiated TEM disks were shipped to Risø National Laboratory for microstructural examination. The TEM disks were electrochemically thinned to perforation at room temperature using a solution of 25% H_3PO_4, 25% ethylene glycol and 50% water with an applied potential of 11 V. The microstructures were examined using a combination of weak beam (WB) and bright field (BF) imaging techniques on a JEOL-2000 FX electron microscope operating at 200 kV. Foil thicknesses were determined by thickness fringe techniques (WB for small defect clusters, BF for network dislocations and dislocation loops) or, in the case of voids, stereo pair analysis. Dislocation loops and defect cluster densities were corrected for invisible defects, according to the $g \cdot b$ criterion. The nature of the resolvable dislocation loops was determined using conventional inside/outside contrast techniques at a minimum of two different diffraction vectors each at two different zone axes. The pure copper specimen irradiated at 420°C was not available for examination in the present study. The tensile properties of companion pure Cu specimens from the two irradiation capsules are summarized elsewhere [18].

3. Results

3.1. 210°C irradiated microstructure

Void formation was not observed in any of the specimens irradiated at 210°C. Instead, a high density of small defect clusters was observed in all of the specimens irradiated at 210°C. The defect cluster density was $8.0 \pm 1.0 \times 10^{23}$ m^{-3}, and the mean image width was 3.0 nm in all specimens. About 90% of the defect clusters were resolvable as SFTs, independent of alloy composition. It is worth noting that defect cluster patterning or wall formation was not evident in any of the specimens.

Fig. 1 shows the dislocation loop microstructure in several of the irradiated specimens. The number density

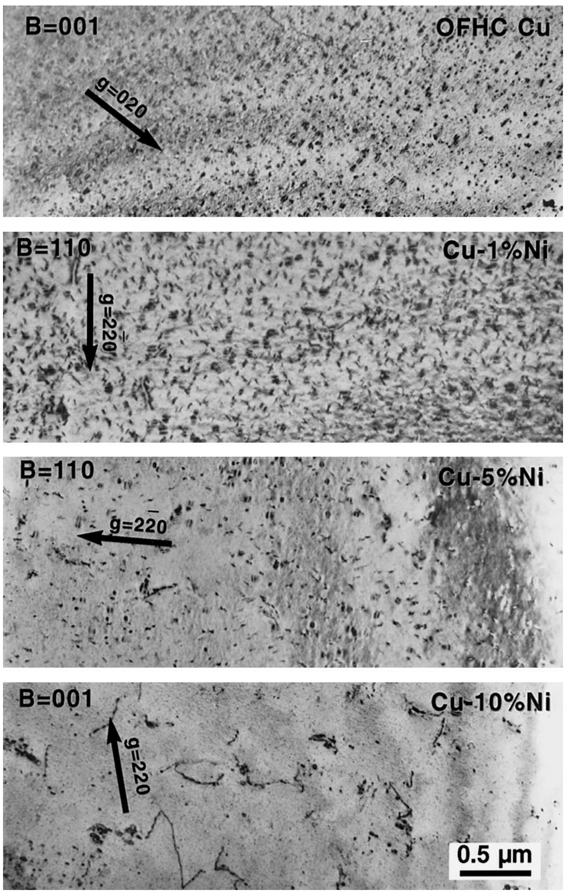

Fig. 1. Dislocation loop microstructure in copper and Cu–Ni alloys irradiated to 13.5 dpa at 210°C.

of 'resolvable' ($d > 5$ nm) loops was maximized in specimens with an initial Ni content of 1%. Since ~1.4% Ni and ~0.5% Zn were produced via transmutation reactions during irradiation, neutron irradiation microstructural data on truly 'pure' Cu are not available from this study. The 'resolvable' dislocation loops had habit planes of {1 1 1} and {1 1 0}. Analysis of the loops indicated that the Burgers vectors were predominantly $a/2\ \langle 1\,1\,0\rangle$ and that the loops were of interstitial type. Therefore, it appears that the small 'black spot' defect clusters (mainly SFTs) are vacancy-type, whereas the larger defect clusters (loops) are interstitial-type, in agreement with previous reports [19,20]. Fig. 2 summarizes the effect of initial Ni content on the small ('black spot') defect cluster and resolvable ($d > 5$ nm) dislocation loop density of specimens irradiated at 210°C.

The decrease in dislocation loop density for initial Ni contents >1% (Fig. 2) was accompanied by a modest increase in network dislocation density. The network dislocation density was 1.5×10^{12} m^{-2} for copper specimens with initial Ni contents up to 1% and gradually increased to 4.5×10^{12} m^{-2} for Cu–10%Ni.

3.2. 420°C irradiated microstructure

A very low density of small defect clusters (5.0×10^{20} m^{-3}, three orders of magnitude lower than at 210°C) was observed in all specimens irradiated at 420°C. The average image width of these defect clusters was ~3.0 nm, similar to what was observed at 210°C. Nearly 100% of these small defect clusters were resolvable as SFTs. The number density of resolvable dislocation loops was too low to be accurately measured. The network dislocation density was 1×10^{12}–3×10^{12} m^{-2}, with no systematic dependence on solute content.

The dominant microstructural feature in all of the specimens irradiated at 420°C was the formation of a moderate density of large voids. A void denuded zone with an average half-width of 2 μm was observed along the grain boundaries of all specimens. Fig. 3 shows typical low-magnification images of void denuded zones at grain boundary triple points in Cu–1%Ni and Cu–10%Ni. The void distribution was very heterogeneous in the matrices of the specimens containing up to 5% Ni. The void density in adjoining regions (with no apparent influence from grain boundaries) often varied by a factor of 10, which made it difficult to quantify the void swelling.

In the specimens with 0.17–2% initial Ni contents, a 'peak swelling zone' that was ~10 μm wide was observed next to the grain boundary denuded zone. Both the void size and density were larger in the peak swelling zone compared to the center of the grain. The peak swelling zone was most pronounced in the Cu–1%Ni specimen. Fig. 4 shows an example of the void denuded and peak swelling zones adjacent to a grain boundary in Cu–

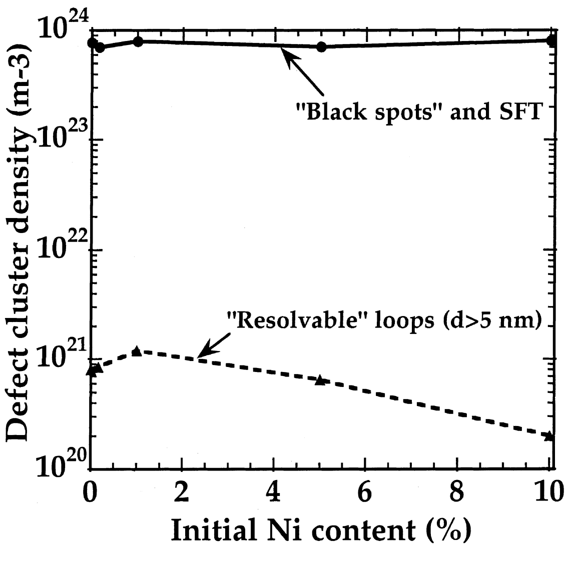

Fig. 2. Effect of initial Ni content on the defect cluster densities of Cu–Ni alloys irradiated to 13.5 dpa at 210°C.

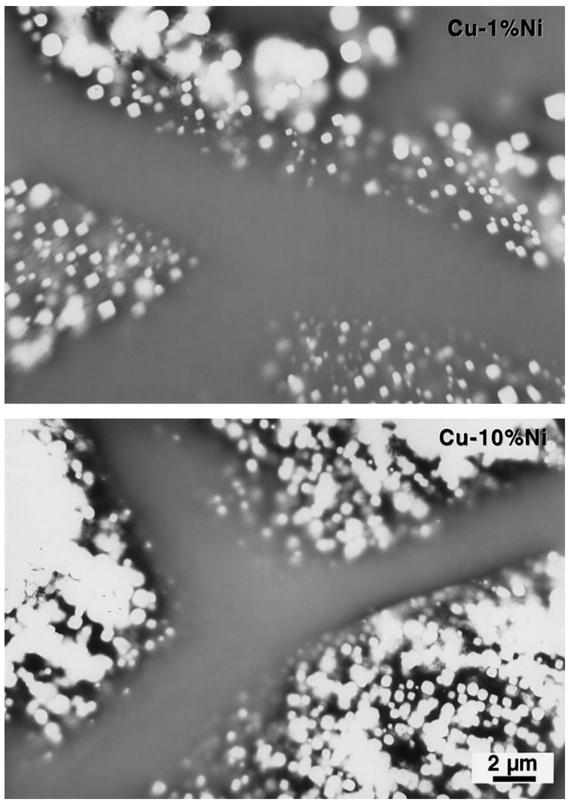

Fig. 3. Heterogeneous void swelling behavior associated with grain boundaries in Cu–Ni alloys irradiated to 14.9 dpa at 420°C.

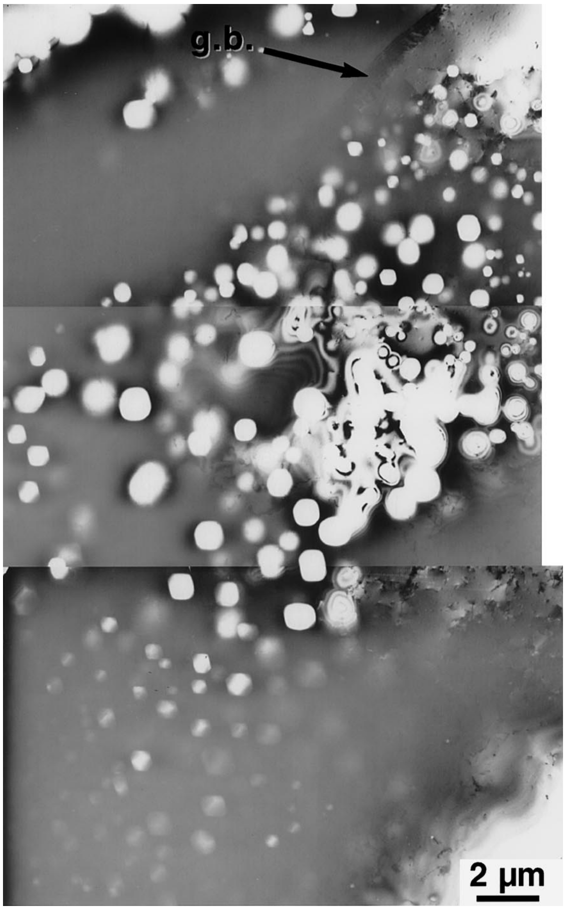

Fig. 4. Void denuded and peak swelling zones adjacent to a grain boundary in Cu–1%Ni irradiated to 14.9 dpa at 420°C.

1%Ni. Very little void swelling was detected in the grain interior (lower right region of Fig. 4), due to a sharp decrease in the void size compared to the peak swelling zone. The void swelling in the peak swelling zone was ~31% (2.1% dpa^{-1}) in this specimen. The swelling in the peak zone of other specimens containing up to 2% Ni was ~20%. Fig. 5 summarizes the void size and density in irradiated Cu–Ni alloys measured at a distance of 4–8 µm from grain boundaries (i.e., within the peak swelling zone). The void diameter decreased and the void density increased as the initial Ni content was increased from 0.17% to 1%. The void size was constant for 1–10% Ni. The void density achieved a maximum at 1% Ni and was independent of Ni content for 2–10% Ni.

The Cu–10%Ni specimen exhibited more spatially uniform void swelling compared to the other specimens. The Cu–10%Ni specimen did not exhibit a clear peak swelling zone near the grain boundaries, and the swelling was ~18% over most of the grain interior. A striking feature that was only observed in Cu–10%Ni was the partial ordering of the voids along ⟨1 1 0⟩ crystallographic directions. Fig. 6 shows an example of this partial void ordering. Further results on the void alignment in Cu–10%Ni, including Hough transform analysis of the void ordering, will be presented elsewhere [21]. There have been only a few observations of void superlattice formation in fcc metals, including aluminum, nickel and stainless steel (see reviews in [22,23]).

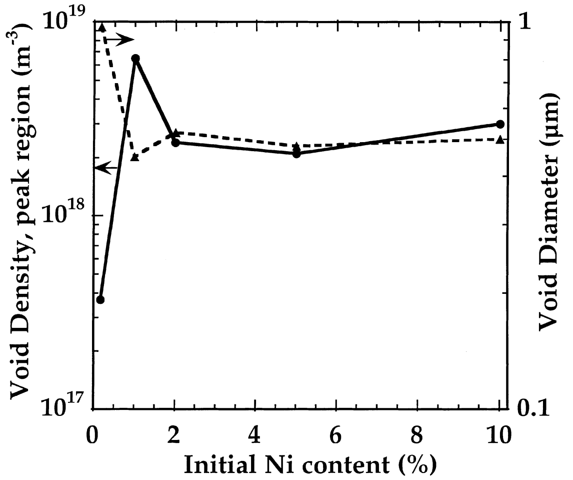

Fig. 5. Void size and density vs. initial Ni content for the peak swelling regions in specimens irradiated to 14.9 dpa at 420°C.

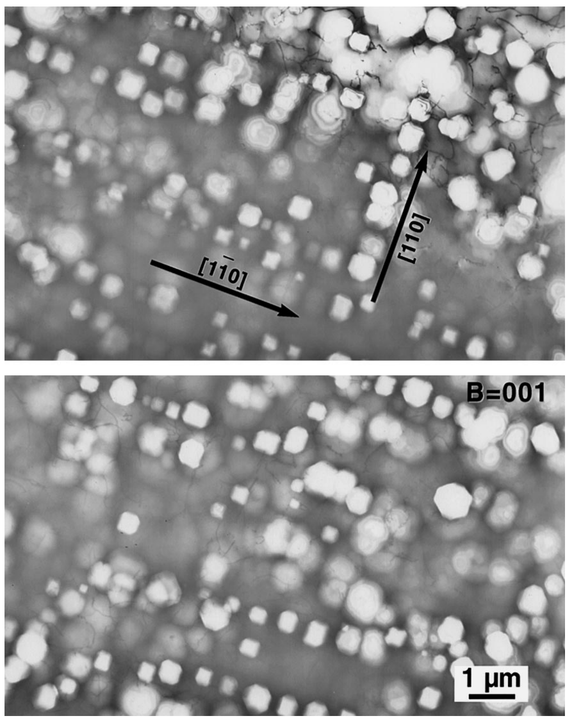

Fig. 6. Void alignment along ⟨1 1 0⟩ crystallographic directions in Cu–10%Ni irradiated to 14.9 dpa at 420°C.

4. Discussion

The present high-dose irradiation results suggest that the lower temperature limit for void formation in fission-neutron-irradiated copper is at least 210°C. Previous neutron irradiation studies have generally found that void formation does not occur in copper irradiated at 180–200°C [24–29], whereas voids are observed after irradiation at 220–230°C [24,25,27,30]. In contrast, Shimomura et al. [31] reported void formation for copper irradiated at 200°C, whereas Labbe et al. [32] did not observe void formation in pure copper for a nominal irradiation temperature as high as 220°C. A recent positron annihilation investigation of copper irradiated with fission neutrons at 200°C to 0.3 dpa found a complete absence of voids or microvoids [33]. Void formation has been observed at a temperature as low as 182°C in Cu–B specimens which generated ~100 appm He during the irradiation [34].

Since both the overall density of 'black spot' defect clusters and the fraction of visible SFTs were independent of Ni content (up to 10% Ni), this implies that displacement cascade production is similar in Cu and Cu–Ni alloys. Unfortunately, irradiated 'pure' Cu is not available for comparison at these neutron irradiation conditions, since ~1.4% Ni and ~0.5% Zn were produced in all specimens during the HFIR irradiation. About 90% of the small defect clusters were resolvable as SFTs in the present study, independent of the initial Ni solute content. Previous work at lower temperatures (25–130°C) indicated that the SFT fraction was lower in irradiated Cu–5%Ni compared to pure copper, although the total number density of 'black spot' defect clusters was comparable in the two materials [35,36]. Conversely, Satoh et al. [37] reported that the addition of 2% Ni to copper caused a slight increase in the density and size of SFTs produced during low-dose 14 MeV neutron irradiation at 150–290°C. As an aside, the SFT densities measured for the 210°C and 420°C specimens agree with a previous lower-dose temperature-controlled neutron irradiation study performed at a slightly lower dose rate [27,34].

In contrast to the 'black spot' defect cluster results, the Ni solute has a significant impact on the formation of 'resolvable' ($d > 5$ nm) dislocation loops and voids in irradiated copper. This might be attributable to slight differences in the cascade production (e.g., fraction of di-, tri- and tetra-interstitial clusters) or migration behavior (including solute segregation) of mobile defects in pure Cu vs. Cu–Ni alloys. In agreement with the present results, several previous studies have observed an enhancement in resolvable dislocation loop density in Cu–Ni alloys compared to pure copper [3,6,10,14,36,37].

Defect cluster patterning [23,38] was not observed in any of the specimens irradiated at 210°C. The observed cluster density in the present study (8×10^{23} m^{-3}) is near the 'saturation' limit obtained in lower-dose irradiation studies performed near room temperature. Therefore, it is difficult to conceive how patterning would occur in neutron-irradiated copper specimens at lower temperatures since the average defect cluster size and density would be anticipated to be similar to those observed in the present study. As discussed elsewhere [39], the only irradiation condition which has produced defect cluster patterning in a bulk copper specimen is 3 MeV H^+ irradiation [23]. This suggests that defect cluster patterning is not a fundamental self-organization phenomenon in irradiated copper but, instead, requires specific primary knock-on atom spectrum and/or other experimental conditions.

The void swelling in the specimens irradiated at 420°C is rather heterogeneous compared to previous neutron irradiation studies on Cu and Cu–Ni alloys performed at 400–420°C [2,3,27]. The average void density measured in the peak swelling region adjacent to the grain boundary denuded zone (Fig. 5) is in rough agreement with previous studies. However, the previous neutron irradiation studies [2,3] have observed a larger difference in void density for the Cu–Ni alloys vs. pure copper than shown in Fig. 5. The 2 μm width of the void denuded zone at grain boundaries is in agreement with previous observations at lower doses [27] and corresponds to about three times the spacing between voids.

The observation of a peak swelling zone next to the grain boundary denuded zone has previously been observed in neutron-irradiated Cu, Al and stainless steel [40–42]. The presence of the peak swelling zone (which was most pronounced in Cu–1%Ni) can be explained by 1-D gliding interstitial clusters with a typical mean free path of ~10 μm [43–45]. The width of the peak swelling zone was ~10 times the 0.8 μm average distance between voids. Previous studies have found that the swelling peaks at a distance from the grain boundary of $\sim 10\ \lambda_v$, and that the peak swelling zone width is $\sim 20\ \lambda_v$, where λ_v is the mean spacing between voids [41]. The reason why the peak swelling zone was most pronounced in the alloys containing 0.17–2% Ni is most likely associated with the large grain size in these alloys (~100–150 μm). The peak swelling zone was not observed in the Cu–10%Ni specimen since the grain size (27 μm) was comparable to twice the width of the peak swelling zone, i.e., the high swelling zone filled essentially all of the grain interior.

Although gas bubble superlattice formation has been observed in helium-implanted copper and other metals, void ordering has not been previously observed in irradiated copper or its alloys [22,46]. The partial void ordering along ⟨1 1 0⟩ directions in Cu–10%Ni irradiated at 420°C may be due to 1-D gliding interstitial clusters, as proposed in the production bias model [45]. Further experimental work is needed to determine whether partial void ordering can occur in copper and copper alloys at other irradiation conditions.

The most likely explanation for the high swelling in the Cu–10%Ni grain interiors compared to the other alloys is that its relatively small grain size (27 μm) is comparable to the width of the peak swelling zone (∼10 μm). Previous studies have found that Ni solute additions cause a significant reduction in the void density of irradiated copper [1–3]. In contrast, the highest void density in the grain interiors is observed in Cu–10%Ni in the present study. In addition to grain size effects, the high helium concentration in the Cu–10%Ni specimen (∼22 appm), compared to the other specimens, is a possible contributor to the relatively high matrix void density in Cu–10%Ni.

5. Conclusions

Addition of >1% Ni appears to have a minor effect on the displacement cascade collapse in copper, based on the similarities in the total defect cluster and SFT densities of irradiated specimens initially containing 0.17–10% Ni. A strict comparison with pure Cu irradiation behavior was not possible in this study due to the production of ∼1.4% Ni and 0.5% Zn from transmutation reactions. Defect cluster patterning is not observed in any of the Cu alloys irradiated at 210°C and is not considered to be a fundamental self-organization phenomenon in neutron-irradiated copper.

In contrast, Ni additions have a significant impact on dislocation loop and void evolution. This implies that either the defect production (e.g., size distribution of clustered point defects) or migration behavior (including solute segregation) of mobile defects is different in Cu vs. Cu–Ni alloys. The dislocation loop density and 'peak swelling zone' is maximized for copper containing ∼1% initial Ni solute. The presence of the peak swelling zone adjacent to the grain boundary void denuded zone in copper containing $\leqslant$2% Ni and the partial ordering of voids in Cu–10%Ni can be explained by the production bias model (1-D transport of interstitial clusters).

Acknowledgements

This research was sponsored in part by the Office of Fusion Energy Sciences, US Department of Energy, under contract DE-AC05-00OR22725 with UT-Battelle, LLC, and partly funded by the European Fusion Technology Programme. The authors thank Janet Pawel-Robertson for assistance with the irradiation and capsule disassembly, Gary Parks for specimen sorting and J. Lindbo for TEM specimen preparation.

References

[1] J.L. Brimhall, H.E. Kissinger, Radiat. Eff. 15 (1972) 259.
[2] B.N. Singh, A. Horsewell, D.S. Gelles, F.A. Garner, J. Nucl. Mater. 191–194 (1992) 1172.
[3] T. Muroga, N. Yoshida, J. Nucl. Mater. 212–215 (1994) 266.
[4] H. Watanabe, F.A. Garner, J. Nucl. Mater. 212–215 (1994) 370.
[5] T. Muroga, H. Watanabe, N. Yoshida, H. Kurishita, M.L. Hamilton, J. Nucl. Mater. 225 (1995) 137.
[6] T. Muroga, H. Watanabe, N. Yoshida, J. Nucl. Mater. 258–263 (1998) 955.
[7] D.J. Mazey, F. Menzinger, J. Nucl. Mater. 48 (1973) 15.
[8] K.-H. Leister, Kernforschungszentrum, Karlsruhe Report KfK-3499, 1983.
[9] T. Muroga, T. Matue, H. Watanabe, N. Yoshida, in: R.K. Nanstad et al. (Eds.), 18th International Symposium on Effects of Radiation on Materials, ASTM STP 1325, American Society for Testing and Materials, West Conshohocken, PA, 1999, p. 991.
[10] B.N. Singh, T. Leffers, P. Barlow, in: Proceedings of the Fifth International Conference on High Voltage Electron Microscopy, Kyoto, Japanese Society of Electron Microscopy, Tokyo, 1977, p. 581.
[11] F.A. Garner, B.N. Singh, in: Fusion Materials Semiannual Progress Report for the Period Ending March 31 1994, DOE/ER-0313/16, Oak Ridge National Laboratory, 1994, p. 364.
[12] F.A. Garner, H.R. Brager, K.R. Anderson, J. Nucl. Mater. 179–181 (1991) 250.
[13] H. Takahashi, S. Ohnuki, T. Takeyama, J. Nucl. Mater. 103&104 (1981) 1415.
[14] T. Muroga, E. Ishimaru, N. Yoshida, in: A.S. Kumar, et al. (Eds.), 16th International Symposium on Effects of Radiation on Materials, ASTM STP 1175, American Society for Testing and Materials, West Conshohocken, PA, 1993, p. 1013.
[15] S.A. Fabritsiev, S.J. Zinkle, B.N. Singh, J. Nucl. Mater. 233–237 (1996) 127.
[16] A.W. Longest, J.E. Pawel, D.W. Heatherly, R.G. Sitterson, R.L. Wallace, in: Fusion Materials Semiannual Progress Report for the Period Ending September 30 1993, DOE/ER-0313/15, Oak Ridge National Laboratory, 1993, p. 23.
[17] L.R. Greenwood, C.A. Baldwin, in: Fusion Materials Semiannual Progress Report for the Period Ending December 31 1997, DOE/ER-0313/23, Oak Ridge National Laboratory, 1997, p. 329.
[18] S.J. Zinkle, L.T. Gibson, in: Fusion Materials Semiannual Progress Report for the Period Ending December 31 1999, DOE/ER-0313/27, Oak Ridge National Laboratory, 1999, p. 163.
[19] M. Rühle, F. Haussermann, M. Rapp, Phys. Stat. Sol. 39 (1970) 609.
[20] B.L. Eyre, J. Phys. F 3 (1973) 422.
[21] S.J. Zinkle, B.N. Singh, N.C.K. Lassen, 2000, to be published.
[22] J.H. Evans, in: D. Walgraef, N.M. Ghoniem (Eds.), Patterns, Defects and Materials Instabilities, Kluwer Academic, Amsterdam, 1990, p. 347.
[23] W. Jäger, H. Trinkaus, J. Nucl. Mater. 205 (1993) 394.

[24] Y. Adda, in: J.W. Corbett, L.C. Ianniello (Eds.), Radiation-induced Voids in Metals, National Technical Information Service, Springfield, VA, 1972, p. 31.
[25] M. Labbe, J.P. Poirier, J. Nucl. Mater. 46 (1973) 86.
[26] N. Yoshida, Y. Akashi, K. Kitajima, M. Kiritani, J. Nucl. Mater. 133&134 (1985) 405.
[27] S.J. Zinkle, K. Farrell, J. Nucl. Mater. 168 (1989) 262.
[28] M. Kiritani, T. Yoshiie, S. Kojima, Y. Satoh, K. Hamada, J. Nucl. Mater. 174 (1990) 327.
[29] M. Kiritani et al., J. Nucl. Mater. 212–215 (1994) 241.
[30] S.J. Zinkle, L.L. Snead, J. Nucl. Mater. 225 (1995) 132.
[31] Y. Shimomura, I. Mukouda, K. Sugio, J. Nucl. Mater. 251 (1997) 61.
[32] M. Labbe, G. Brebec, J.P. Poirier, J. Nucl. Mater. 49 (1973) 232.
[33] M. Eldrup, B.N. Singh, presented at ICFRM9, Colorodo Springs, CO, 10–15 October 1999, submitted to Philos. Mag. A, 2000.
[34] S.J. Zinkle, K. Farrell, H. Kanazawa, J. Nucl. Mater. 168 (1991) 262.
[35] S.J. Zinkle, J. Nucl. Mater. 150 (1987) 140.
[36] S.J. Zinkle, A. Horsewell, B.N. Singh, W.F. Sommer, J. Nucl. Mater. 212–215 (1994) 132.
[37] Y. Satoh, I. Ishida, T. Yoshiie, M. Kiritani, J. Nucl. Mater. 155–157 (1988) 443.
[38] D. Walgraef, J. Lauzeral, N.M. Ghoniem, Phys. Rev. B 53 (1996) 14782.
[39] S.J. Zinkle, L.L. Snead, B.N. Singh, D.J. Edwards, in: Fusion Materials Semiannual Progress Report for the Period Ending September 30 1994, DOE/ER-0313/17, Oak Ridge National Laboratory, 1994, p. 69.
[40] R.E. Stoller, G.R. Odette, J. Nucl. Mater. 154 (1988) 286.
[41] B.N. Singh, S.J. Zinkle, J. Nucl. Mater. 206 (1993) 212.
[42] B.N. Singh, A. Horsewell, J. Nucl. Mater. 212–215 (1994) 410.
[43] H. Trinkaus, B.N. Singh, A.J.E. Foreman, J. Nucl. Mater. 206 (1993) 200.
[44] B.N. Singh, S.I. Golubov, H. Trinkaus, A. Serra, Y.N. Osetsky, A.V. Barashev, J. Nucl. Mater. 251 (1997) 107.
[45] S.I. Golubov, B.N. Singh, H. Trinkaus, J. Nucl. Mater. 276 (2000) 78.
[46] P.B. Johnson, D.J. Mazey, Nature 276 (1972) 595.